A comprehensive study of X-ray supernova remnants in nearby galaxies

Leonidaki [1,2,3], A. Zezas [2], P. Boumis [1]

[1] Institute of Astronomy & Astrophysics, National Observatory of Athens, Athens, Greece
[2] Harvard-Smithsonian Center for Astrophysics, Cambridge, MA, USA
[3] Department of Physics, University of Patras, Rio-Patras, Greece

Introduction

Supernova Remnants (SNRs) are an important component of the X-ray source populations in galaxies (e.g. Blair & Long 1997), especially in luminosities below 10^{37} erg/s. The expanding SNR shocks heat the surrounding interstellar medium (ISM) to X-ray emitting temperatures of 10^6 - 10^7 K. This way SNRs chemically enrich the ISM and provide a significant fraction of the mechanical energy that heats and shapes it. Although it is almost certain that environment plays a major role in the evolution and the multiwavelength properties of SNRs (e.g. Pannuti et al 2007), the details of this connection are poorly understood. In order to address this connection, we initiated an X-ray study of seven nearby star-forming galaxies with high quality Chandra data.

Sample & Data Analysis

Our sample consists of the nearby galaxies (NGC2403, NGC4214, NGC3077, NGC4449, NGC4395, NGC5204 and M81) observed with Chandra and fulfill the following criteria : a) Distance < 5 Mpc, in order to minimize source confusion; b) Inclination < 60 degrees, in order to minimize internal extinction and projection effects; and c) Exposure times long enough to achieve a uniform detection limit of ~10^{36} erg/sec. The X-ray data analysis was performed with the CIAO tool suite version 3.4 and with custom developed scripts. This analysis includes initial cleaning of the data, source detection, photometry and multi-band image extraction. The source detection was performed with wavdetect. In this work we focus only on sources within the D25 area of each galaxy. Source photometry was obtained from regions encompassing at least 90% of the encircled energy in each band, and was corrected for effective area variations over the detector and between different observations of the same object.
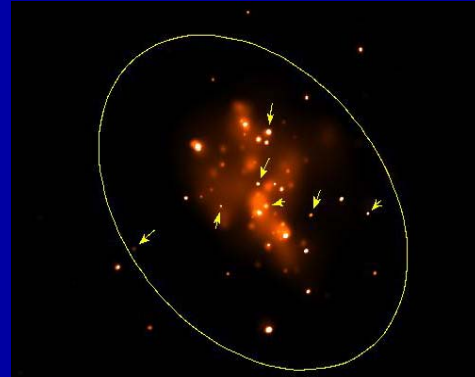

Fig 1 – Smoothed image of NGC4449: The arrows show the X-ray selected SNRs, while the ellipse indicates the D25 region of the galaxy.

Identification of SNRs

We calculated X-ray colours for the detected X-ray sources and created colour-colour diagrams, (e.g. Fig 2), using the BEHR method (Park et al. 2006). On the same plots we added grids for power-law and thermal-plasma models for different temperature (kT), absorbing HI column density (N_H) and photon index (Γ). These diagrams can be used to identify a set of objects for further study (the locus of thermal SNRs is shown by the red circle). In order to verify their nature, we performed spectral fits for all the candidate SNRs with adequate number of counts. We find that 15 sources have X-ray spectra consistent with thermal SNRs based on the presence of a low-temperature thermal-plasma spectrum (e.g. Fig 3). None of these sources has a hard X-ray component. Twenty one additional sources are considered as candidate thermal SNRs based on their soft X-ray colours.
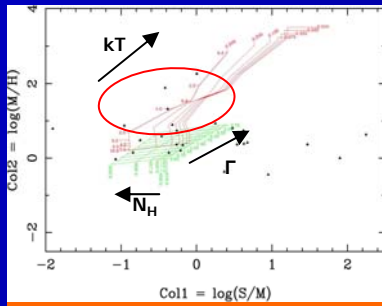

Fig 2: Colour-colour plot for NGC4449. S, M, H are the numbers of counts in the soft (0.1-3.0keV), medium (1.0-2.5keV) and hard band (2.5-8.0keV). Points outside the grids have large errors and/or complex multi-component spectra.
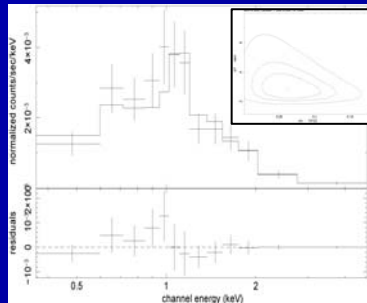

Fig. 3: X-ray spectrum of an SNR in NGC3077, fitted with an apec model. In the insert we show kT-N_H confidence contours at the 1,2 and 3 SIGMA levels.

M81 : a case study

We have also analyzed Chandra archival data for M81 in order to obtain a more complete multi-wavelength image of the SNR populations in this prototypical spiral galaxy. We focused on the central region of the galaxy (covered by the monitoring campaign of Pooley et al.). We detect 120 X-ray sources down to 10^{36} erg/s (Fig. 4), ~ 40 of which are identified as candidate X-ray SNRs based on their X-ray colours. Cross-correlation of the X-ray sources with the optical SNR sample of Matonick et al. (1997) shows that six optically known SNRs have X-ray counterparts, two of which are located within the locus of thermal SNRs on the colour-colour diagram. Grid and their luminosities indicate that they can be X-ray SNRs (Fig. 4).
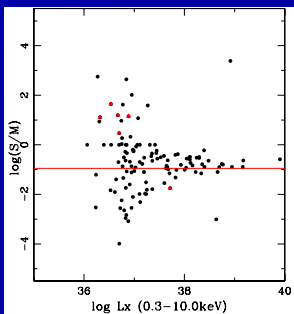

Fig.4: X-ray color - luminosity plot. The red line indicates our 2keV criterion for X-ray selected thermal SNRs (log(S/M)>-0.95). The red points represent X-ray sources associated with optical SNRs in the sample of Mattonick et al.
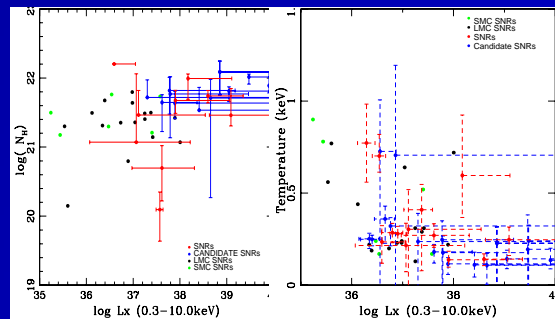

Fig.5: L_x-N_H **plot.** Sources with fixed or unconstrained N_H have not been included.

Fig.6 L_x - kT **plot.** Most of our sample have soft thermal spectra. The sources in Figs 5-6 have 1σ errobars.

Results

In Figs. 5 and 6 we present a plot of the column density (N_H) and the temperature against the absorption-corrected luminosity of the SNRs, based on the parameters from the spectral fits. In the same plots we also show for comparison a sample of Magellanic Cloud (MC) SNRs from the Chandra Supernova Remnant Catalogue. From these plots we see that: (a) the extragalactic SNRs extend the trends of the MC-SNRs to higher luminosities; (b) the majority of our X-ray selected SNRs are within the 0.1 - 1keV range (which is typical for thermal SNRs); (c) we do not find a strong correlation between luminosity and N_H or temperature. Finally, the luminosity distribution of our sample of SNRs (shown in Fig. 7) is fairly flat with a small population of luminous (>10^{38} erg/s) SNRs.

In the case of M81, the poor correlation between X-ray and optical SNRs is in agreement with similar studies in other galaxies (e.g. Pannuti et al. 2007). This is believed to be due to the different evolutionary stages of SNRs probed in optical and X-ray wavebands.

Fig. 7: Luminosity distribution of our sample of X-ray selected SNRs (the first bin is severely affected by incompleteness).

References

Pannuti, T, Schlegel, E. M., Griffith, S.A., 2007, AJ, 210, 1510
Pooley, D., et al.
Blair, W.P. & Long, K.S., 1997, ApJS, 108, 261
Mattonick, D.M. & Fesen, R.A., 1997, ApJS,112, 49
Park, T. et al., 2006, ApJ, 652, 610